BULLETIN OF THE POLISH ACADEMY OF SCIENCES
TECHNICAL SCIENCES, Vol. 71(3), 2023, Article number: e145565
DOI: 10.24425/bpasts.2023.145565

Impact of thermal backfill parameters on current-carrying capacity of power cables installed in the ground

Seweryn SZULTKA[1]*, **Stanislaw CZAPP**[1], and **Adam TOMASZEWSKI**[2]

[1] Faculty of Electrical and Control Engineering, Gdansk University of Technology, Narutowicza 11/12, 80-233 Gdansk, Poland
[2] Institute of Fluid-Flow Machinery, Polish Academy of Sciences, Fiszera 14, 80-231 Gdansk, Poland

Abstract. Proper design of power installations with the participation of power cables buried in homogeneous and thermally well-conductive ground does not constitute a major problem. The situation changes when the ground is non-homogeneous and thermally low-conductive. In such a situation, a thermal backfill near the cables is commonly used. The optimization of thermal backfill parameters to achieve the highest possible current-carrying capacity is insufficiently described in the standards. Therefore, numerical calculations based on computational fluid dynamics could prove helpful for designers of power cable lines. This paper studies the influence of dimensions and thermal resistivity of the thermal backfill and thermal resistivity of the native soil on the current-carrying capacity of power cables buried in the ground. Numerical calculations were performed with ANSYS Fluent. As a result of the research, proposals were made on how to determine the current-carrying capacity depending on the dimensions and thermal properties of the backfill. A proprietary mathematical function is presented which makes it possible to calculate the cable current-carrying capacity correction factor when the backfill is used. The research is expected to fill the gap in the current state of knowledge included in the provisions of standards.

Key words: current-carrying capacity; numerical simulations; power cables; thermal analysis.

1. INTRODUCTION

The current-carrying capacity of underground power cables depends on several factors. In addition to the known factors related to the construction of power cables, e.g. cross-sectional area of conductors, an equally important factor is the thermal resistivity of the ambient soil [1, 2]. In turn, thermal resistivity of the soil depends mainly on the moisture content as well as on the density and conductivity of the grain from which it is composed [3]. In practice, depending on specific conditions of laying power cables in the ground, maintaining a constant and preferably relatively low value of thermal resistivity of the soil poses a technical problem [4]. The lower the thermal resistivity of the soil, the more effective the heat transfer by means of conduction in it. Therefore, it is possible to increase the current-carrying capacity of underground power cables by lowering thermal resistance of the surrounding soil. However, in practice, it is difficult to keep constant and low thermal resistivity of the soil, as it is affected, for example, by the migration of moisture and soil diversity along the power cable line length [4–8]. An important problem described by scientists is also the formation of a dry zone around the cables (due to the cables being highly loaded and hot), which results in a local increase of thermal resistivity of the soil. To reduce or even avoid the aforementioned undesired effect, thermal backfill can be used. It is characterized by low thermal resistivity and good immunity to moisture migration and drying out. In addition, thermal backfill is a stable mechanical basis for power cable operation and protection against external pressure and threats [3]. The economic dimension of the use of thermal backfill is an important argument for investors and designers [2, 9]. In such cases, detailed analysis related to the current-carrying capacity of the power cable line laid in the designed thermal backfill should be carried out. Determining the current-carrying capacity of a power cable line placed directly in the ground (without backfill) is not a major problem – the provisions given in standards [10–13] act as the design guidelines in that case. The obtained current-carrying capacity results are accurate and constitute a verification of numerical models [5, 14, 15]. However, determining the current-carrying capacity in cable systems with thermal backfill is not easy due to the fact that standards cannot be applied directly. Standards [10–13] are based on the Neher-McGrath method [16], which does not provide accurate results for installations with thermal backfill [5, 14, 15]. In those cases, the solution to the problem may be the use of numerical calculations, an approach which was successfully implemented in this article.

To date, many scientists have studied the current-carrying capacity of power cables with thermal backfill. Paper [15] presents multivariate numerical calculations of power cables arranged in a backfill, however, the accuracy/verification of the calculation model was not specified. In [17], an interesting conclusion is given that the geometry of the backfill is more important than the effect of placing the cable in the backfill.

*e-mail: seweryn.szultka@pg.edu.pl

Manuscript submitted 2022-08-24, revised 2023-03-01, initially accepted for publication 2023-03-02, published in June 2023.

However, that conclusion was based on a small number of experimental attempts. Among the materials used for backfills, betonite has the best properties related to thermal conductivity [8]. In [18], the depth and the distance between the cables were examined, but the geometry of the thermal backfill was not analyzed. The authors of article [19] report that backfill dimensions have a significant effect on current-carrying capacity but no explanation for this is provided. In turn, articles [20] and [21] include the results of the research concerning the assessment of the effect of thermal backfill conductivity on current-carrying capacity, but without investigating the influence of backfill geometry.

With reference to the literature review, this article analyzes the issues of thermal resistivity of the soil and thermal backfill as well presents an assessment of the influence of thermal backfill geometry on the current-carrying capacity of the power cable line. The issues described below constitute an actual and important technical problem that currently poses a challenge for designers and investors. The essence of the problem is the use of appropriate thermal backfill in undergrounded power cable systems, where soil replacement is often a necessity to ensure appropriate mechanical and thermal conditions for the operation of cable lines [9,22]. The use of thermal backfill with appropriate parameters, which is the subject of the research reported in this article, has a positive impact on optimal operation and distributed control of various types of power networks [23]. It will also improve the reliability of power supply required by energy producers and grid operators [24].

2. DESCRIPTION OF THE COMPUTING MODEL

2.1. Assumptions for the numerical model

The article reports the calculations of thermal states of a low-voltage power cable line. The model of the power line has a relatively simple structure, which facilitates numerical calculations, at the same time not worsening the quality of the thermal analysis results obtained. The article analyses a power cable line with 3 single-core copper conductors with a cross-sectional area of 35 mm^2 each, placed in PVC insulation and a jacket/sheath. Figure 1 shows the type of power cables being analyzed.

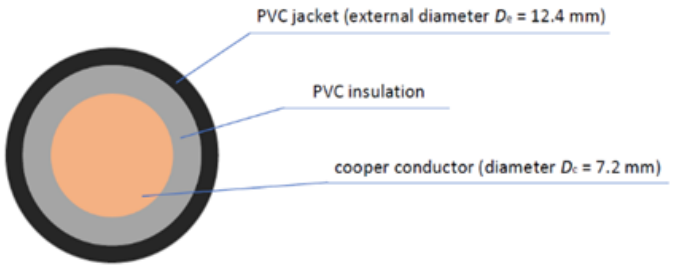

Fig. 1. Cross-section view of the type of power cable being analyzed

In order to verify the numerical model with the provisions of standard [13], a series of calculations were performed. The calculations concerned a relatively simple case with the mentioned power cable line laid directly in the ground. This method of numerical model verification is widely accepted [15]. For this purpose, the numerical model shown in Fig. 2 was implemented in the ANSYS Fluent software.

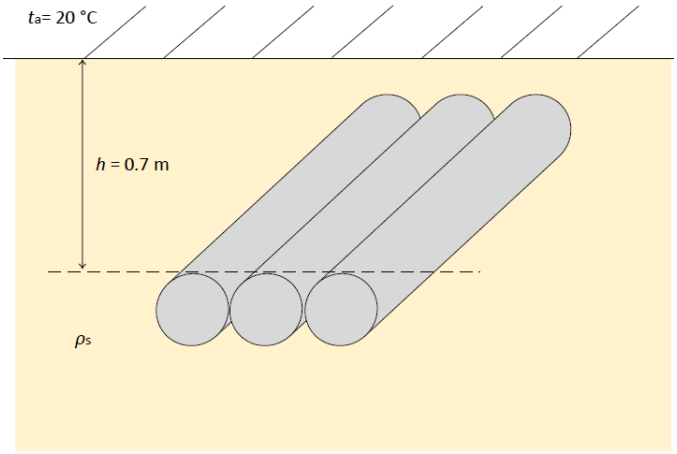

Fig. 2. Simplified model of the analyzed cable line

Power cables in the touching arrangement are laid directly in the ground with variable thermal resistivity ρ_s. The laying depth h of the power cable line is 70 cm. Air temperature above the ground, t_a, is 20°C. The calculations of the current-carrying capacity I_z of the power cable line were performed for 3 different values of soil thermal resistivity. The results are presented in Table 1. For numerical calculations, the value of the current-carrying capacity was calculated from equation (1):

$$I_z = \sqrt{\frac{q_{\text{Joule}} \cdot \pi \cdot D_c}{R_{\text{AC}}}}, \tag{1}$$

where: I_z – current-carrying capacity, A, q_{Joule} – Joule's heat flux density, W/m^2, R_{AC} – power cable resistance for AC current, Ω, D_c – copper conductor diameter, mm.

Table 1
Model verification results

ρ_s [K·m/W]	I_z [A]	
	Numerical simulations	PN-HD 60364-5-52
0.5	219.4	207
1.0	169.8	165
2.0	127.4	124

The Joule's heat value was determined iteratively for each simulation performed. The condition for completing the iteration was for the power cable line to reach the maximum permissible temperature (for PVC insulation it is 70°C).

Two-dimensional geometries of the system were used in numerical simulations and two-dimensional analysis has been performed. The structure of the cable system is presented in Fig. 2 (without backfill) and Fig. 7 (with backfill). The domain was

created in DesignModeler software and it was divided into separate sections, each for different material. The "share topology" method was used during the process of geometry creation, which allows to avoid the manual process of interface definition and two adjacent curves were then treated as a single one, when mesh was imported to the solver software. The computational domain around this structure was discretized in order to perform the finite element method (FEM) calculations. The computational mesh (see Fig. 3) consisted of approx. 400 000 square elements. It was imported into ANSYS Fluent, after which the numerical model was created.

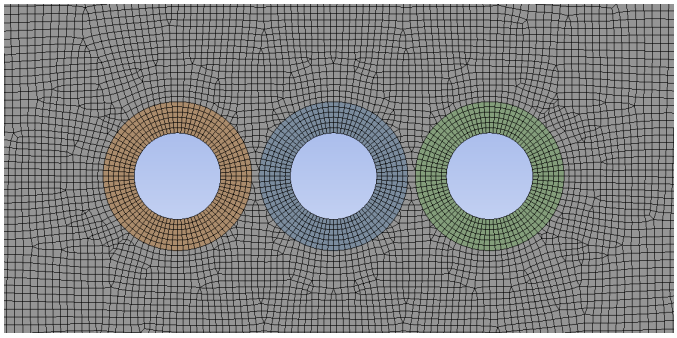

Fig. 3. Computational mesh around power cables

The steady-state simulation of heat transfer between the power cables and the surrounding material was performed. The energy equation was activated and density as well as thermal properties of different materials (among others: thermal conductivity, specific heat) were included in the model. On the upper surface of the ground, the wall boundary condition was set with the option of convective heat transfer coefficient $\alpha_{conv} = 15$ W/m^2·K. This value corresponds to no wind conditions or to such when the wind speed is low, which is expected to occur most of the time at ground level. This is the most disadvantageous variant from the point of view of heat transfer, as it may cause overheating of power cables. In the lower part of the ground (under the cables), the wall boundary condition was also chosen, and the temperature was set at 8°C. This temperature can be considered constant regardless of the weather and season. On the inner part of the cable's insulation, the wall boundary condition with heat flux option was chosen. The heat flux was increased until the maximum temperature in the system reached 70°C (max permissible temperature for cable insulation). The second order discretization scheme was set for energy. Only the energy equation was solved in ANSYS Fluent, so the equations of flow and turbulence were disabled. The convergence criterion was set to "none" and during the calculation process the chart of residual of energy equation was observed. The calculations were performed until this residual stopped changing.

The obtained results of the simulation tests, shown in Table 1, are characterized by high convergence with the results given by standard PN-HD 60364-5-52 [13]. The convergence is between 3% and 5%, while the accuracy of the results from the standard according to the comments contained therein is ±5%. Thus, the applied initial calculation model can be used for further calculations.

The temperature distributions around the cables in the analyzed cases are shown in: Fig. 4, Fig. 5 and Fig. 6.

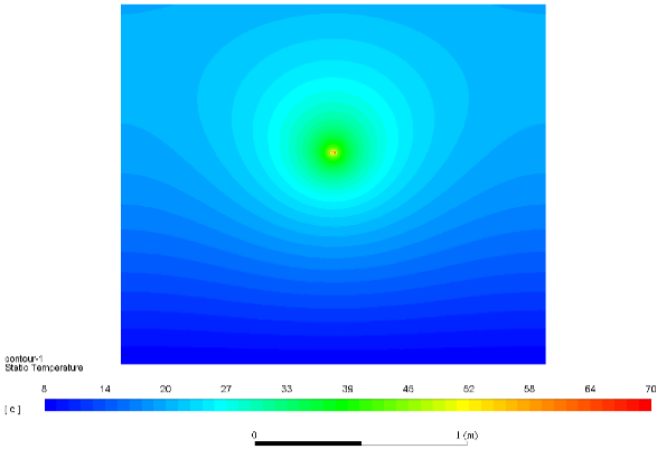

Fig. 4. Temperature distribution for power cable line buried in the ground with thermal resistivity ρ_s of 0.5 (K·m)/W

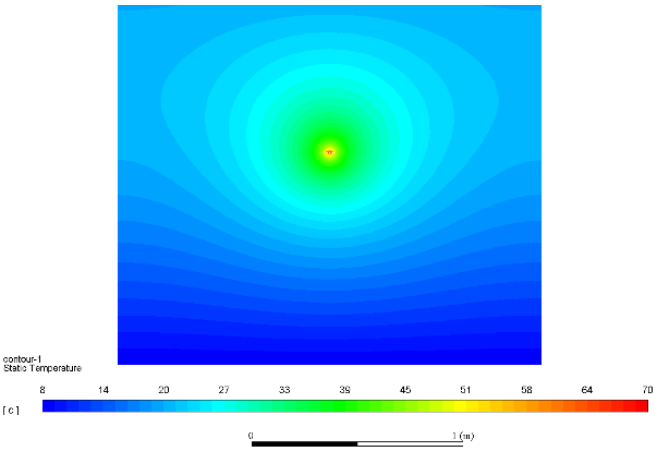

Fig. 5. Temperature distribution for power cable line buried in the ground with thermal resistivity ρ_s of 1.0 (K·m)/W

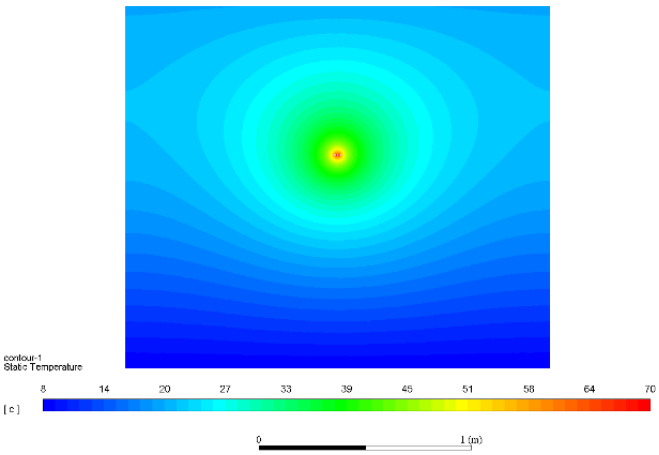

Fig. 6. Temperature distribution for power cable line buried in the ground with thermal resistivity ρ_s of 2.0 (K·m)/W

2.2. Computer model with thermal backfill

The numerical analyses with variable parameters of the power cable line thermal backfill were prepared in ANSYS Fluent software according to the graphic interpretation presented in a simple manner in Fig. 7. The model shown in Fig. 7 is an expansion of that shown in Fig. 2 by means of including variable thermal backfill. The calculations performed for the power cable line with thermal backfill took into account: geometric dimension b, thermal resistivity ρ_b of thermal backfill and thermal resistivity ρ_s of soil, considered in Section 2.1 of this article.

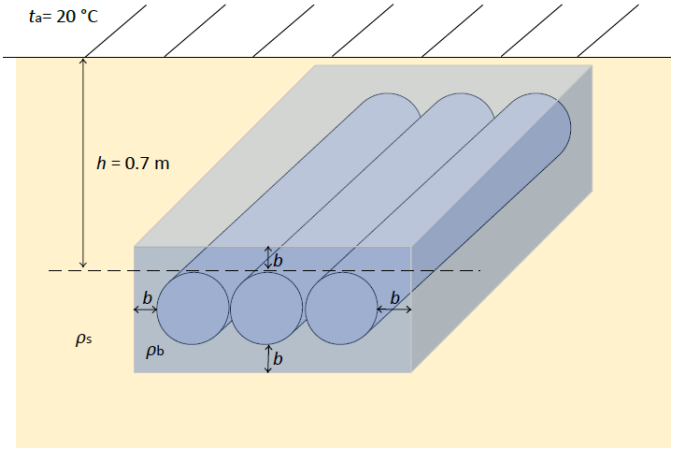

Fig. 7. Simplified model of the analyzed power cable line with thermal backfill

A mixture of sand and cement with thermal resistivity of 0.75 or 1.0 (K·m)/W is very often used as thermal backfill material. The results of multi-criteria calculations are presented in Table 2.

In the calculations, three different values of dimension b were considered: 10, 20 and 30 cm. The thermal resistivity of soil, ρ_s, was equal to: 0.5, 1.0 and 2.0 (K·m)/W, while the thermal resistivity of backfill, ρ_b, was 0.75 or 1.0 (K·m)/W. Selected temperature distributions are presented in Figs. 8–12. In the figures, the black lines composing the rectangle around the cable line indicate the area of backfill.

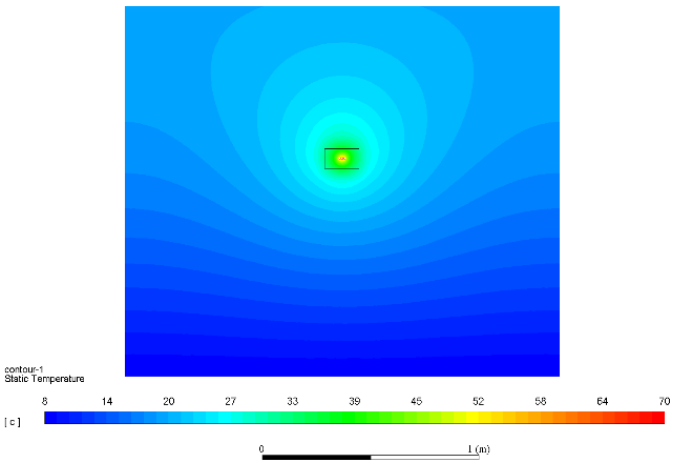

Fig. 8. Temperature distribution for the following case: $\rho_s = 0.5$ (K·m)/W, $\rho_b = 1.0$ (K·m)/W, $b = 10$ cm, $I_z = 187.6$ A

Table 2
Results and parameters of multi-criteria calculations

b [cm]	ρ_s [K·m/W]	ρ_b [K·m/W]	I_z^* [A]
10	0.5	0.75	200.3
10	1.0	0.75	179.7
10	2.0	0.75	152.8
10	0.5	1.0	187.6
10	1.0	1.0	169.8
10	2.0	1.0	146.7
20	0.5	0.75	197.6
20	1.0	0.75	183.2
20	2.0	0.75	161.5
20	0.5	1.0	181.2
20	1.0	1.0	169.8
20	2.0	1.0	152.8
30	0.5	0.75	195.7
30	1.0	0.75	184.7
30	2.0	0.75	166.5
30	0.5	1.0	178.2
30	1.0	1.0	169.8
30	2.0	1.0	156.3

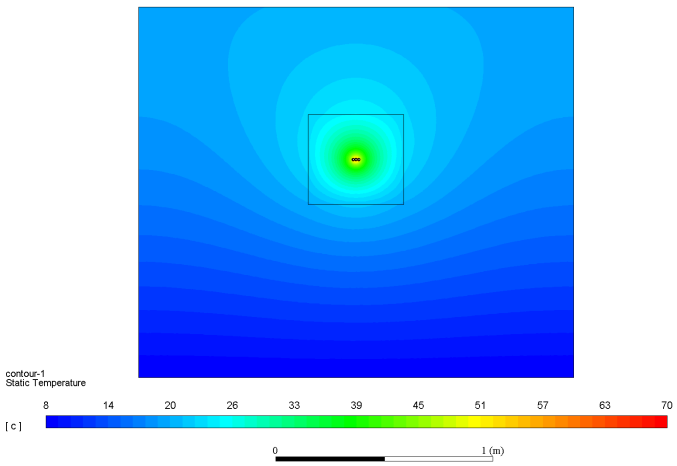

Fig. 9. Temperature distribution for the following case: $\rho_s = 0.5$ (K·m)/W, $\rho_b = 1.0$ (K·m)/W, $b = 20$ cm, $I_z = 181.2$ A

As can be seen in Fig. 8–12, the increase in thermal resistivity of the soil significantly influences temperature distribution around the power cable line. This can be seen when comparing Fig. 10 and Fig. 11, where Fig. 11 shows the temperature distribution for higher thermal resistivity of the soil (larger heated area) than in the case of soil resistivity of 0.5 (K·m)/W (Fig. 10).

To assess the influence of the geometry and thermal resistivity of the backfill on the current-carrying capacity, the de-

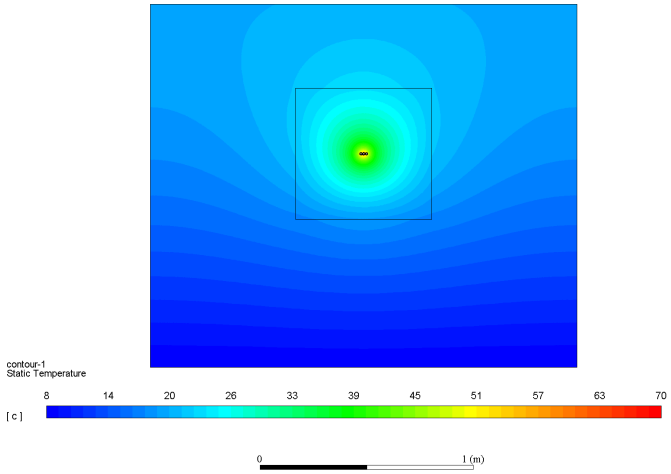

Fig. 10. Temperature distribution for the following case: $\rho_s = 0.5$ (K·m)/W, $\rho_b = 1.0$ (K·m)/W, $b = 30$ cm, $I_z = 178.2$ A

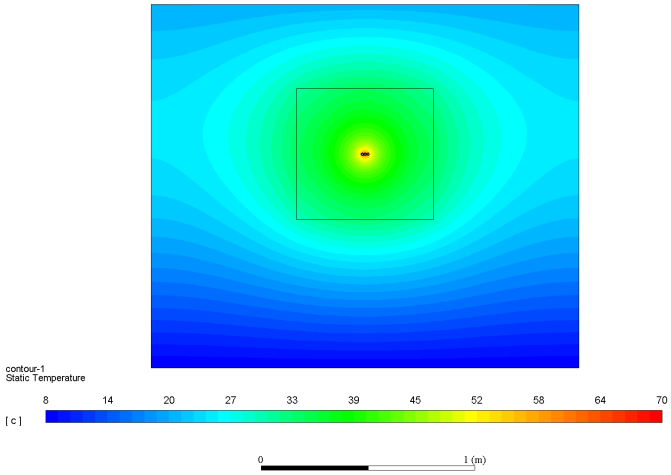

Fig. 11. Temperature distribution for the following case: $\rho_s = 2.0$ (K·m)/W, $\rho_b = 1.0$ (K·m)/W, $b = 30$ cm, $I_z = 156.3$ A

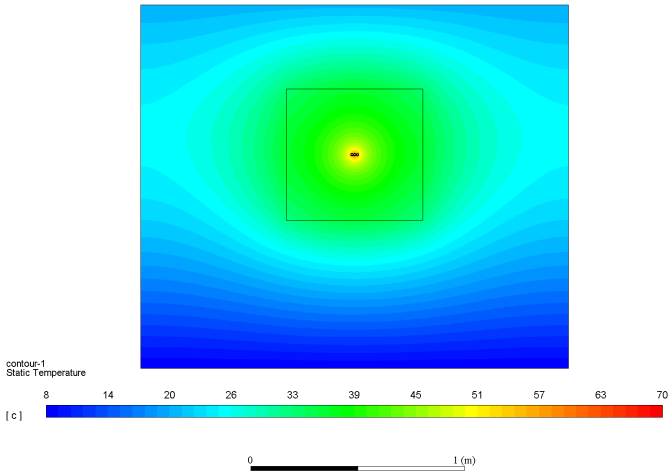

Fig. 12. Temperature distribution for the following case: $\rho_s = 2.0$ (K·m)/W, $\rho_b = 0.75$ (K·m)/W, $b = 30$ cm, $I_z = 166.5$ A

pendence diagram shown in Fig. 13 was prepared. As can be seen, for thermal resistivity of soil $\rho_s = 0.5$ (K·m)/W, the use of thermal backfill reduces the permissible load of the power cable line regardless of the value of thermal resistivity of the backfill. However, the use of thermal backfill in power cables placed in the ground above $\rho_s = 1.0$ (K·m)/W increases their current-carrying capacity. For these cases, with the increase in the amount of thermal backfill and with the decrease in its thermal resistivity, the current-carrying capacity increases. The points of intersection with the ordinate axis (I_z axis) marked in Fig. 13 constitute the simulation results presented in Table 1.

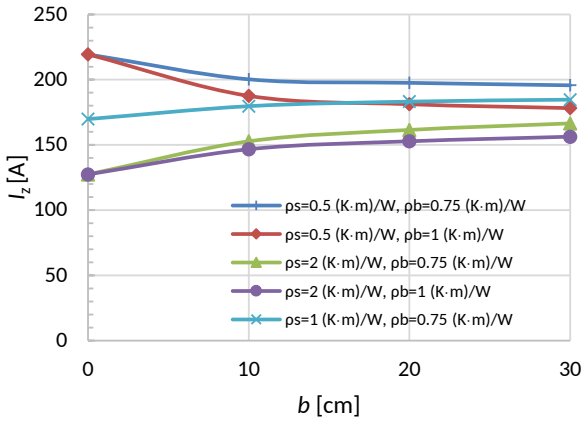

Fig. 13. Current-carrying capacity as function of dimension and type of thermal backfill

In order to generalize the results obtained, the value of the current-carrying capacity correction factor was introduced according to equation (2):

$$I_{\text{cor}} = \frac{I_z^*}{I_z}, \tag{2}$$

where: I_{cor} – correction factor, –, I_z^* – current-carrying capacity with thermal backfill, A, I_z – current-carrying capacity without thermal backfill, A. I_z^* and I_z are the values of current described in Table 2 and Table 1, respectively. For the cases without backfill, the values of the factor are equal to one. A graphical list of correction factor values for the considered cases is presented in Fig. 14.

Figure 14 also includes linear functions approximating the obtained factor values depending on backfill geometry. After analyzing the results depicted in Fig. 14, mathematical analysis of the obtained values was performed, as a result of which a universal formula to calculate the correction factor is proposed in equation (3):

$$I_{\text{cor}} = \left(-0.0021 \cdot \left(\frac{\rho_s}{\rho_b}\right)^2 + 0.018 \cdot \frac{\rho_s}{\rho_b} - 0.0159\right) \cdot b + 1. \tag{3}$$

Table 3 presents a comparison of the factor values obtained from computer simulations (2) and from the proposed universal mathematical equation (3). High convergence of relevant results

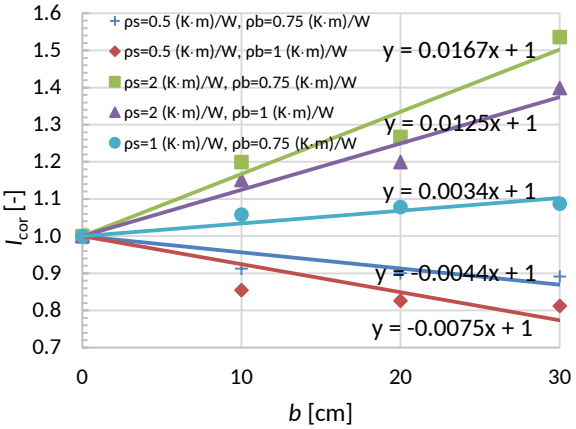

Fig. 14. Correction factor (I_{cor}) as function of dimension (b) and type of thermal backfill (variable thermal resistivity ρ_b)

can be observed. The correction factor applied allows to determine the current-carrying capacity for a cable line placed in the ground of known thermal resistivity with a backfill of known thermal resistivity and geometry. Equation (3) applies to b values of up to 30 cm. From a practical point of view, this value is definitely sufficient for common use.

Table 3
Examples of correction factor values

ρ_s/ρ_b [–]	b [cm]	I_{cor} [A]		Difference [%]
		According to (2)	According to (3)	
0.5/0.75	30	0.892	0.855	4.15
0.5/1.0	20	0.826	0.8515	3.09
2.0/0.75	30	1.536	1.515	1.37
2.0/1.0	10	1.151	1.117	2.95

3. CONCLUSIONS

The presented simulation studies have shown that thermal backfill may clearly improve the current-carrying capacity of power cable lines. In the cases of significant difference in thermal resistivity between the native soil and the backfill, the increase of this capacity is very high. For the cable line analyzed in the article, it was around 50% as compared to the solution without backfill. The proposed mathematical formula for calculation of the current-carrying capacity correction factor can be used by designers of cable lines where backfill is to be used. Further simulation studies are aimed at validating this function for other geometries of thermal backfill.

REFERENCES

[1] F. De León, "Major factors affecting cable ampacity," in Power Engineering Society General Meeting,2006. IEEE, 2006, p. 6, doi: 10.1109/PES.2006.1708875.

[2] S. Czapp and F. Ratkowski, "Optimization of Thermal Backfill Configurations for Desired High-Voltage Power Cables Ampacity," *Energies*, vol. 14, no. 5, p. 1452, 2021, doi: 10.3390/en14051452.

[3] J. Sundberg, "Evaluation of thermal transfer processes and backfill material around buried high voltage power cables," Report / Department of Civil and Environmental Engineering, Chalmers University of Technology, vol. 5, 2016,

[4] Z.R. Radakovic, M.V. Jovanovic, V.M. Milosevic, and N.M. Ilic, Application of earthing backfill materials in desert soil conditions," *IEEE Trans. Ind. Appl.*, vol. 51, no. 6, pp. 5288–5297, 2015, doi: 10.3390/app11125623.

[5] O.E.-S. Gouda, G.F.A. Osman, W.A. Salem, and S.H. Arafa, "Cyclic loading of underground cables including the variations of backfill soil thermal resistivity and specific heat with temperature variation," *IEEE Trans. Power Deliv.*, vol. 33, no. 6, pp. 3122–3129, 2018, doi: 10.1109/TPWRD.2018.2849017.

[6] O.E. Gouda, A.Z. El Dein, and G.M. Amer, "Effect of the formation of the dry zone around underground power cables on their ratings," *IEEE Trans. Power Deliv.*, vol. 26, no. 2, pp. 972–978, 2010, doi: 10.1109/TPWRD.2010.2060369.

[7] O.E. Gouda and A.Z. El Dein, "Improving underground power distribution capacity using artificial backfill materials," *IET Gener. Transm. Distrib.*, vol. 9, no. 15, pp. 2180–2187, 2015, doi: 10.1049/iet-gtd.2015.0274.

[8] C. Gomes, C. Lalitha, and C. Priyadarshanee, "Improvement of earthing systems with backfill materials," in *2010 30th International Conference on Lightning Protection (ICLP)*, 2010, pp. 1–9, doi: 10.1109/ICLP.2010.7845822.

[9] A. Cichy, B. Sakowicz, and M. Kaminski, "Economic optimization of an underground power cable installation," *IEEE Trans. Power Deliv.*, vol. 33, no. 3, pp. 1124–1133, 2017, doi: 10.1109/TPWRD.2017.2728702.

[10] IEC 60287-1-1:2006 Electric cables – Calculation of the current rating – Part 1–1 Current rating equations (100% load factor) and calculation of losses – General.

[11] IEC 60287-2-1:2015 Electric cables – Calculation of the current rating – Part 2–1 Thermal resistance – Calculation of the thermal resistance."

[12] IEC 60287-3-1:1999 Electric cables – Calculation of the current rating – Part 3–1 Sections on operating conditions – Reference operating conditions and selection of cable type.

[13] PN-HD 60364-5-522011 Instalacje elektryczne niskiego napięcia – Część 5–52 Dobór i montaż wyposażenia elektrycznego – Oprzewodowanie (*eng*. Electrical Low Voltage Installations – Part 5–52 Selection and installation of electrical equipment – Wiring).

[14] L. Ramirez and G.J. Anders, "Cables in Backfills and Duct Banks – Neher/McGrath Revisited," *IEEE Trans. Power Deliv.*, vol. 36, no. 4, pp. 1974–1981, 2020, doi: 10.1109/TPWRD.2020.3017616.

[15] F. De Leon and G.J. Anders, "Effects of backfilling on cable ampacity analyzed with the finite element method," *IEEE Trans. Power Deliv.*, vol. 23, no. 2, pp. 537–543, 2008, doi: 10.1109/TPWRD.2008.917648.

[16] J.H. Neher and M.H. McGrath, "The calculation or the temperature rise and load capability of cable systems," Trans. Am. Inst. Electr. Eng. Part III: Power Appar. Syst., vol. 76, pp. 752-764, 1957, doi: 10.1109/AIEEPAS.1957.4499653.

[17] K.E. Saleeby, W.Z. Black, and J.G. Hartley, "Effective thermal resistivity for power cables buried in thermal backfill," *IEEE Trans. Power Appar. Syst.*, no. 6, pp. 2201–2214, 1979, doi: 10.1109/ TPAS.1979.319419.

[18] A.A. Al-Dulaimi, M.T. Güneşer, and A.A. Hameed, "Investigation of Thermal Modeling for Underground Cable Ampacity Under Different Conditions of Distances and Depths," in *2021 5th International Symposium on Multidisciplinary Studies and Innovative Technologies (ISMSIT)*, 2021, pp. 654–659, doi: 10.1109/ISMSIT52890.2021.9604732.

[19] K. Charerndee, R. Chatthaworn, P. Khunkitti, A. Kruesubthaworn, A. Siritaratiwat, and C. Surawanitkun, "Investment Cost Analysis with Structural Design of Concrete Duct Bank Power Cables," in *IOP Conference Series: Materials Science and Engineering*, vol. 897, no. 1, 2020, doi: 10.1088/1757-899X/897/1/012007.

[20] Y. Yang, Q. Wang, and Z. Liu, "Simulation of Underground Cable Temperature Distribution Based on Multiphysics Modeling," in *2021 11th International Conference on Power, Energy and Electrical Engineering (CPEEE)*, 2021, pp. 26–31, doi: 10.1109/CPEEE51686.2021.9383365.

[21] O.E. Gouda, A.Z. El Dein, and G.M. Amer, "The effect of the artificial backfill materials on the ampacity of the underground cables," in *2010 7th International Multi-Conference on Systems, Signals and Devices*, 2010, pp. 1–6, doi: 10.1109/SSD.2010.5585551.

[22] M. Eckhardt, H. Pham, M. Schedel, and I. Sass, "Investigation ofFluidized Backfill Materials for Optimized Bedding of Buried Power Cables," in *EGU General Assembly Conference Abstracts*, 2021, pp. 5654, doi: 10.5194/egusphere-egu21-5654.

[23] M. Parol, P. Kapler, J. Marzecki, R. Parol, M. Polecki, and L Rokicki, "Effective approach to distributed optimal operation control in rural low voltage microgrids," *Bull. Pol. Acad. Sci. Tech. Sci.*, vol. 68, no. 4, pp. 661–668, 2020, doi: 10.24425/bpasts.2020.134178.

[24] I. Wasiak and Z. Hanzelka, "Integration of distributed energy sources with electrical power grid," *Bull. Pol. Acad. Sci. Tech. Sci.*, pp. 297–309, 2009, doi: 10.2478/v10175-010-0132-1.